



Article

Influence of Electromagnetic Activation of Cement Paste and Nano-Modification by Rice Straw Biochar on the Structure and Characteristics of Concrete

Alexey N. Beskopylny ^{1,*}, Sergey A. Stel'makh ², Evgenii M. Shcherban' ³, Levon R. Mailyan ⁴, Besarion Meskhi ⁵, Alla S. Smolyanichenko ⁶, Valery Varavka ⁷, Nikita Beskopylny ⁸ and Natal'ya Dotsenko ²

¹ Department of Transport Systems, Faculty of Roads and Transport Systems, Don State Technical University, 344003 Rostov-on-Don, Russia

² Department of Construction of Unique Buildings and Structures, Don State Technical University, 344003 Rostov-on-Don, Russia

³ Department of Engineering Geology, Bases, and Foundations, Don State Technical University, 344003 Rostov-on-Don, Russia

⁴ Department of Roads, Don State Technical University, 344003 Rostov-on-Don, Russia

⁵ Department of Life Safety and Environmental Protection, Faculty of Life Safety and Environmental Engineering, Don State Technical University, 344003 Rostov-on-Don, Russia

⁶ Department of Water Supply and Sewerage, Don State Technical University, 344003 Rostov-on-Don, Russia

⁷ Research and Education Center "Materials", Don State Technical University, 344003 Rostov-on-Don, Russia

⁸ Department Hardware and Software Engineering, Don State Technical University, 344003 Rostov-on-Don, Russia

* Correspondence: besk-an@yandex.ru; Tel.: +7-8632738454



Citation: Beskopylny, A.N.; Stel'makh, S.A.; Shcherban', E.M.; Mailyan, L.R.; Meskhi, B.; Smolyanichenko, A.S.; Varavka, V.; Beskopylny, N.; Dotsenko, N. Influence of Electromagnetic Activation of Cement Paste and Nano-Modification by Rice Straw Biochar on the Structure and Characteristics of Concrete. *J. Compos. Sci.* **2022**, *6*, 268. <https://doi.org/10.3390/jcs6090268>

Academic Editor: Jian-Guo Dai

Received: 14 August 2022

Accepted: 9 September 2022

Published: 12 September 2022

Publisher's Note: MDPI stays neutral with regard to jurisdictional claims in published maps and institutional affiliations.



Copyright: © 2022 by the authors. Licensee MDPI, Basel, Switzerland. This article is an open access article distributed under the terms and conditions of the Creative Commons Attribution (CC BY) license (<https://creativecommons.org/licenses/by/4.0/>).

Abstract: One main global problem is the accumulation of a large amount of agricultural waste. This problem causes environmental pollution and requires an immediate comprehensive solution. The purpose of this study was scientific substantiation and experimental testing, at the micro- and macro levels, of the joint influence of electromagnetic activation of cement paste and nano-modification by rice straw biochar on the strength and strain properties of concrete. In addition to standard methods, the methods of electromagnetic activation, scanning electron microscopy, and energy dispersive spectrometry were used. The results of the joint influence of electro-magnetic activation and nano-modification by rice straw biochar on the strength and strain characteristics of concrete were experimentally verified and confirmed by microstructure analysis. Electromagnetic treatment of the cement paste increased the compressive strength, axial compressive strength, tensile strength in bending, and axial tensile strength of concrete. The best performance was demonstrated by electromagnetically-activated concrete containing 5 wt.% rice straw biochar. Strength characteristics increased from 23% to 28% depending on the type of strength, ultimate tensile strains decreased by 14%, and ultimate compressive strains by 8% in comparison with the control concrete composition. Replacing part of the cement with 10 wt.% and 15 wt.% rice straw biochar led to a strong drop in strength characteristics from 14 to 34% and an increase in strain characteristics from 9 to 21%. Scanning electron microscopy showed a denser and more uniform structure of electromagnetically activated samples.

Keywords: composite materials; rice straw; biochar; nanomodified concrete; vortex layer apparatus; electromagnetic treatment

1. Introduction

Modern manufacturing and agricultural sectors are characterized by many global problems that are typical for most countries of the world. One of them can be called the accumulation of a large amount of waste of various origins, one of the main types of which is agricultural waste. Such a problem requires an immediate solution due to

environmental pollution, and it is obvious that such a solution should be comprehensive. That is, it is not enough to simply dispose of agricultural waste. It is necessary to consider the most expedient technology for its utilization with possible applications in various industries [1–3]. One of the most demanded industries as an opportunity to dispose of various types of waste is the construction industry and, in particular, the production of building materials, products, and structures.

The current trend in the modern construction industry is the use of the most environmentally friendly materials and technologies to reduce the degree of negative impact of anthropogenic activities on the environment, while using various kinds of preexisting waste [4–7]. At the same time, the actively developing hydraulic engineering construction requires higher quality indicators of concrete structures compared to civil engineering, due to the increased load on them, as well as a highly aggressive environment both inside and outside the structures. It is known that the strength properties of concrete depend both on the quality of the components themselves and on the properties of the binders—cement and fillers, as well as the mixing water [8–12]. In turn, the characteristics of the cement itself are largely influenced by the degree of grinding carried out in various ways. The range of technologies associated with the processing of solids, divided into separate processes, is presented in Figure 1 [13].

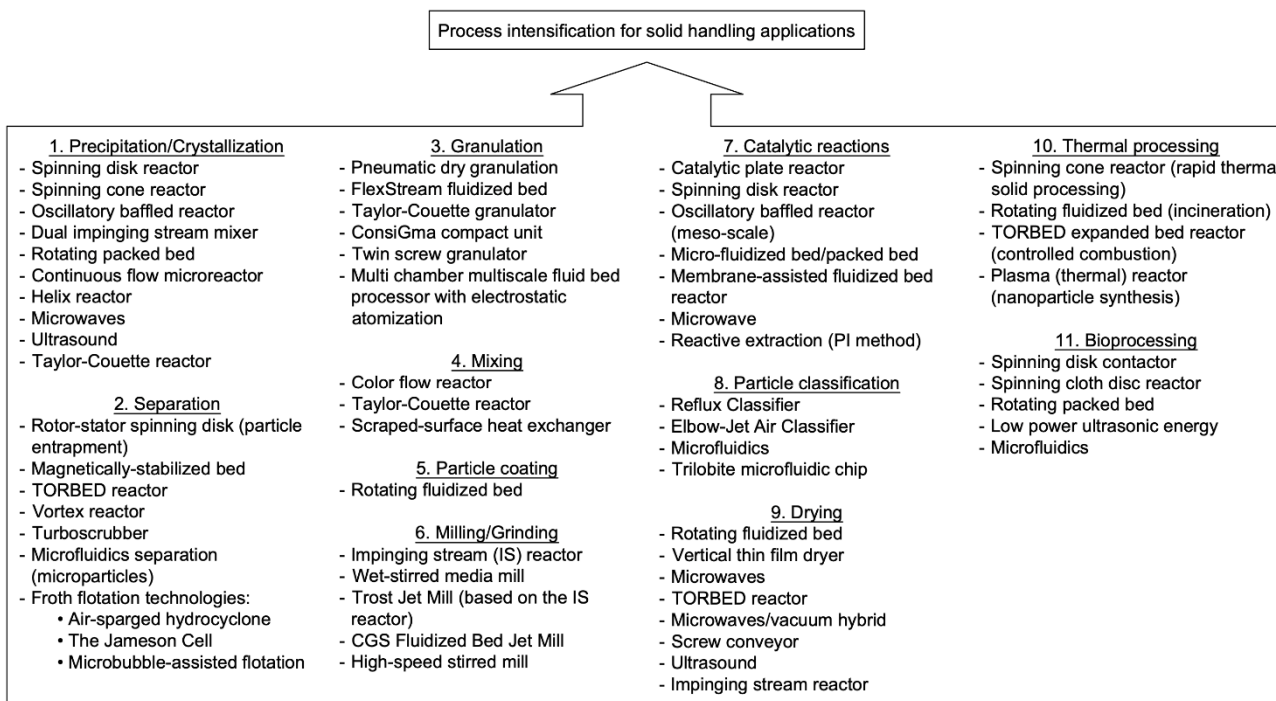


Figure 1. Modern intensive technologies and methods for processes associated with solids processing devices [13].

Among the technical solutions that have emerged in the cement industry are vertical roller mills, high-pressure press rolls, and a combination of press rolls and ball mills [14]. An annular roller mill is also known, which not only allows the processing of the material with its optimal performance, but is also highly energy efficient equipment [15]. These aggregates can be classified depending on how the material is destroyed—compression, shear, friction, or impact. However, it is often difficult to separate the different ways of applying force, since at least two of them act simultaneously in the unit. In addition, during the destruction of the material, three types of fragmentation are distinguished, namely grinding due to abrasion, chipping, and volumetric destruction, which are realized simultaneously to one degree or another. Thus, it is obvious that the grinding mechanism and the type of destruction affect the shape of the product particles [16–21]. In turn, the morphology of cement particles determines its strength characteristics [22]. In addition,

the disintegration of concrete can be used to restore its properties, thereby allowing the use of old cement on construction sites in whole or in part. Studies have shown that the preparation of cement samples in the DESI-16C disintegrator (from old and new cement) made it possible to increase several strength characteristics, however, without changing the chemical properties of materials [23]. Also, disintegration allows the use of non-standard additives of natural and synthetic origin as a filler. For example, in [24], limestone, which is disintegrated together with clinker, was an additive in concrete, since it belongs to local materials in Tunisia, which make it possible to reduce the cost of the concrete manufacturing process without reducing the strength characteristics, but in a limited amount. A relationship has also been established between the quality of grinding and the strength characteristics of concrete. In one study [25], a relationship was established between the crushing of fillers of natural origin—gravel and pebbles with a fraction of 4–8 mm and 10–14 mm, respectively and the strength of concrete. According to the analysis carried out, the sample with gravel showed higher strength characteristics. Natural fillers for partial replacement of Portland cement in concrete also include clays [26], whose chemical and pozzolanic activity was increased by grinding in a planetary ball mill.

One of the most effective methods for increasing the resistance of concrete structures to various kinds of loads is the modification of concrete with carbon fibers. In studies [27,28], it was confirmed that the obtained self-compacting fiber-reinforced concrete with carbon fibers has higher strength characteristics than samples with low porosity and high adhesion, which were achieved by grinding the surface of the samples. Along with inorganic fillers for fiber-reinforced concrete, organic material can also be used, for example, straw processed into ash. The work [29] presents studies on the “potential of concrete with wheat straw ash” and silicon dioxide for several indicators, including CO₂ emission.

In the mid 1970s, the first vortex layer apparatus (VLA) was invented, in which needles moving under the influence of a rotating magnetic field were used as grinding bodies. These devices make it possible to carry out such operations as grinding, mechanical activation of starting materials, and, in particular, the increase of the reactivity of the processed material in subsequent processes and reactions. In addition, VLA devices allow mixing solid bulk materials, liquids and gases, as well as dry grinding of solids, chemical reactions, and changes in the chemical and physical properties of materials [30,31]. The vortex layer apparatus proved to be a very effective way to activate mineral binders [32]. In the apparatus, the processed material is affected by a complex of acoustic, mechanical, electrical, magnetic, thermal, radiation, and chemical effects that change the physicochemical properties of materials [33–37]. In order to improve the efficiency of processing binders on the apparatus of the vortex layer, a formula was obtained for the dependence of the number of collisions of ferromagnetic particles on the number and speed of their movement, the filling factor of the working chamber of the apparatus [38]. Also, the vortex layer apparatus made it possible to significantly increase the strength and deformation characteristics of lightweight fiber-reinforced concrete with a minimum processing time of only 85 s [31]. In studies [39,40], the effect of mixing with magnetized water in a vortex layer installation on the compressive strength of concrete, workability and the required cement content was considered. As a result, a reduction in cement content of 7.5% was confirmed for concrete samples prepared with magnetized mixing water compared to samples prepared with ordinary non-magnetized water. If we consider the disintegration of mineral binders in a vortex layer installation from the point of view of mechanical action, then it is necessary to note the possibility of grinding the material to nanoparticles. For example, it is known that the grinding of Portland cement in a ball mill to nanosizes makes it possible to achieve a 32% increase in compressive strength and reduce the initial setting time to 30 min with 50% replacement of the initial binder with nanocement [41].

The use of waste from the agricultural complex in construction, namely the waste of rice straw, as well as husks, is currently a topical issue, which is confirmed by numerous studies [42–56]. In them, rice straw and husk biochar was used as a replacement for 2%

to 30% of the cement. At the same time, a dosage of 2% to 10% of rice straw ash (RSA) provided the best concrete strength values.

Thus, after conducting a literature review on the existing methods of agricultural waste disposal with its processing into building materials, it is possible to formulate a scientific research deficit. The scientific novelty of this article is the investigation of the mechanisms that occur during the formation of the microstructure and properties of concrete obtained by means of electromagnetic activation and nanomodification with agricultural waste, namely rice straw biochar. Rational dosages are also given with confirmation and scientific justification of this rationality for the highest quality structure and operational reliability of such concretes. The practical significance of the study is to obtain ready-made concretes recommended for use in a wide range of construction areas: in civil, social, industrial, agricultural, and other construction. Thus, the purpose of the study is scientific substantiation and experimental testing, at the micro- and macro levels, of the joint influence of electromagnetic activation and nano-modification by rice straw biochar on the strength and strain properties of concrete.

The objectives of the study are to establish the optimal dosage of the nanomodifier and the optimal combination of electromagnetic activation and modification modes, to identify fundamental relationships between the formation of the microstructure and the formation of the properties of new concretes, and to develop proposals for the applied industry based on the results obtained.

2. Materials and Methods

Portland cement CEM I 42.5 N (OAO Novoroscement, Novorossiysk, Russia) without additives was used as the main binder. The primary properties, chemical and mineralogical mixture of Portland cement are given in Tables 1 and 2.

Table 1. Properties of Portland cement.

Property	Value
Specific surface, cm^2/g	3124
Normal consistency, %	25.5
Density, kg/m^3	3112
Setting time, hour-min.	
- start	2–20
- end	3–25
Compressive strength at the age of 28 days, MPa	43.7
Tensile strength in bending at the age of 28 days, MPa	5.3

Table 2. Mineralogical composition of Portland cement.

Cement Type	C_3S	C_2S	C_3A	C_4AF
CEM I 42.5 N	68.9	13.4	6.3	11.4

Granite crushed stone (Yug-Nerud, Pavlovsk, Russia) was used as a coarse aggregate. Properties of the crushed stone are presented in Table 3.

Quartz sand was used as a fine aggregate (Arkhipovsky quarry, Arkhipovskoe village, Russia). Properties of the sand are given in Table 4.

The quality indicators of the original rice straw biochar and rice straw biochar with electromagnetic processing are shown in Table 5 and in Figures 2 and 3.

Table 3. Properties of the granite crushed stone.

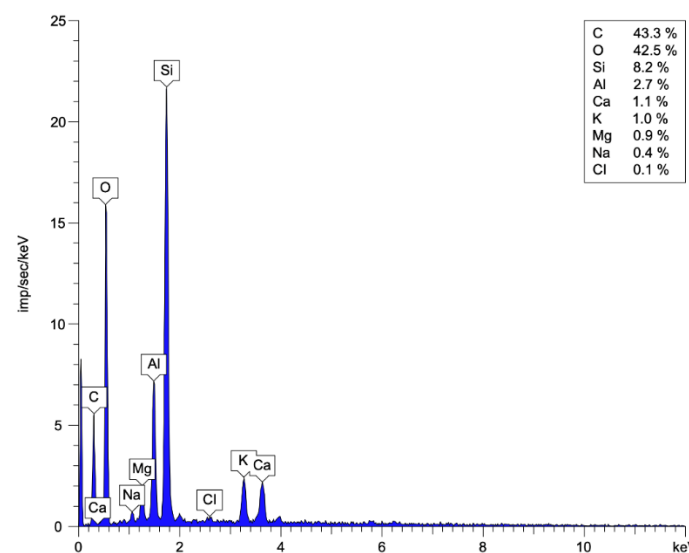
Characteristic Name	Value
Fraction size	10–20
Bulk density, kg/m ³	1456
True density, kg/m ³	2670
Crushability, % by weight	11.2
The content of flaky grains, % by weight	6.4

Table 4. Properties of the quartz sand.

Grain composition of sand	Indicator Title	Indicator Value					
	Sieve size, mm	2.5	1.25	0.63	0.315	0.16	<0.16
	Parttial rests, %	3.0	3.9	6.1	38.6	46.8	1.7
	Full rests, %	3.0	6.8	13.0	51.5	98.3	
Fineness modulus							1.73
Content of Dust and Clay Particles, %							0.25
True grain density, kg/m ³							2665
Bulk density, kg/m ³							1428

Table 5. Chemical composition of the obtained samples of activated rice straw biochar and without activation by electromagnetic treatment.

Sorbent Type	C, %	O, %	Si, %	K, %	Ca, %	Mg, %	Na, %	Cl, %	Fe, %	Al, %
Rice straw biochar with electromagnetic treatment [54]	78.5	18.5	2.1	0.5	0.1	0.1	0.1	-	0.1	-
Rice straw biochar without electromagnetic treatment	43.3	42.5	8.2	1.0	1.1	0.8	0.3	0.1	-	2.7

**Figure 2.** Chemical composition of rice straw biochar without electromagnetic treatment.

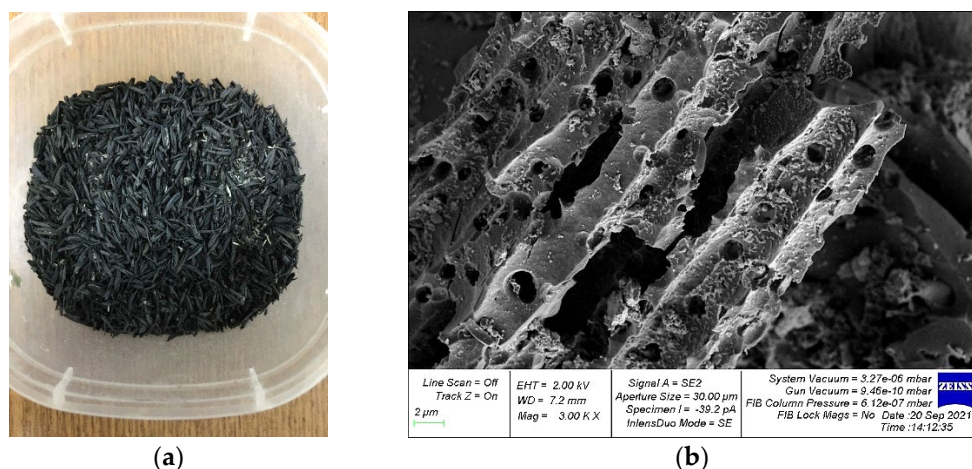


Figure 3. Rice straw biochar (a) appearance; (b) microstructure with a resolution of 1 nm [54].

Table 6 and Figure 2 show that electromagnetic activation changes the chemical composition of rice straw biochar: for example, the proportion of C increased by 35.2%.

Table 6. Compositions of concrete mixes.

Composition Number	Composition Type	Cement, kg/m ³	Water, L/m ³	RSA, kg/m ³
1	Control composition	375	94	0
2	Electromagnetically treated cement paste	375	94	0
3	Electromagnetic treated cement paste with RSA 5% instead of part of the cement	356.3	94	18.7
4	Electromagnetically processed cement paste with RSA 10% instead of part of the cement	337.5	94	37.5
5	Electromagnetically treated cement with RSA 15% instead of part of the cement	318.7	94	56.3

The appearance of the raw material for obtaining nanomodified rice straw biochar powder is shown in Figure 3.

"A sample of rice straw biochar is a corpuscular porous body, and individual particles of which have ordered cylindrical pores without a bottom of approximately equal size. The material itself can be directly attributed to nanomaterials with a particle size of 10 to 100 nm" [54].

Rice straw biochar was prepared according to the following method. Rice straw was washed with distilled water, then soaked in an alkali solution for a day, after which it was repeatedly washed with distilled water until a pH of 7.0–8.0 was reached, after which it was dried for 8 h in a ShS-80-01 SPU drying cabinet (Smolensk SKTB SPU, Smolensk at t = 105 °C). The dried straw was carbonized in a muffle furnace at t = 600 °C for 30 min.

Electromagnetic processing was carried out on a process activation unit (UAP) (DSTU, Rostov-on-Don, Russia). This installation has small dimensions and low specific energy consumption, while allowing the changing of the structure and properties of processed materials [54].

The concrete mix manufacturing process included the following main technological steps:

- at the first stage, cement paste was made with the required amount of rice straw biochar additive or without it. Cement and additives were mixed dry automatically in a laboratory concrete mixer for 1 min, and then water was introduced in an amount of 25% by weight of cement. The resulting cement paste was mixed for another 1 min;

- at the second stage, the resulting cement paste was unloaded from the concrete mixer and subjected to electromagnetic processing in the UAP unit [54];
- at the third stage, the treated cement paste was again placed in a concrete mixer, and then fine aggregate and 50% of the remaining mixing water were introduced. This whole mixture was mixed for 1 min;
- the fourth stage included the introduction of coarse aggregate and the remaining mixing water with the mixing of the concrete mixture until a homogeneous state.

The composition of the concrete mixture chosen was the same as in [54]: cement-375 kg/m³; water-210 L/m³, crushed stone-1028 kg/m³; sand-701 kg/m³. The density of the concrete mixture was 2315 kg/m³.

The compositions of all mixtures are summarized in Table 6.

In the course of the research, 5 series of samples were prepared and tested at the age of 28 days: 1 the control composition of the cement mixture and concrete; 2 cement mixture with processing at the process activation unit (UAP) and concrete on this mixture; 3 cement mixture with rice straw biochar filler (5% instead of cement part) with processing at the process activation unit and concrete on this mixture; 4 cement mixture with rice straw biochar filler (10% instead of cement part) with processing at the process activation unit and concrete on this mixture; 5 cement mixture with rice straw biochar filler (15% instead of cement part) with UAP treatment and concrete on this mixture. The test plan is shown in Figure 4.

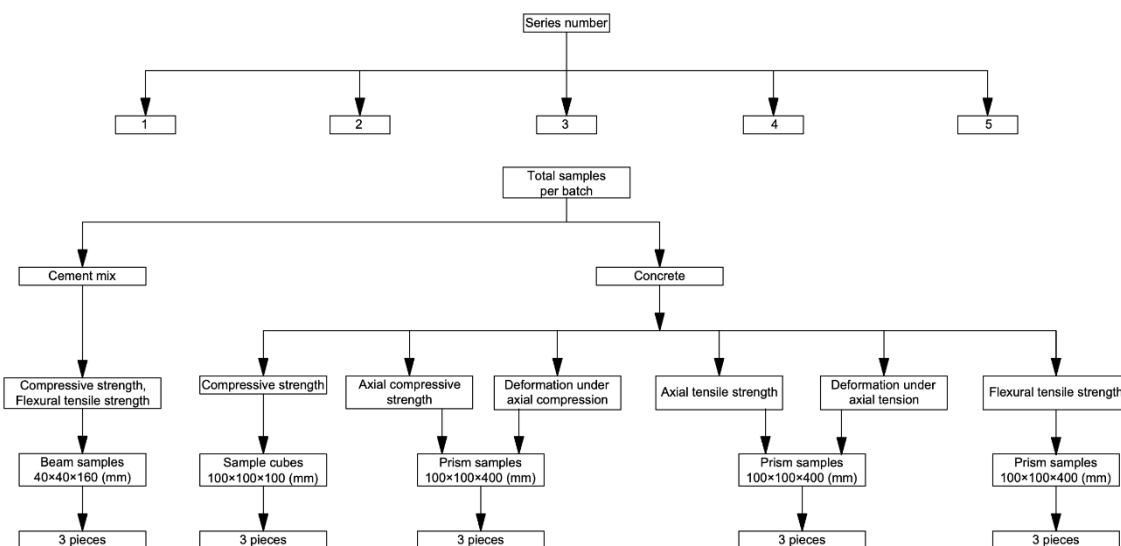


Figure 4. Experimental research program.

In total, 15 specimens of cement paste beams were tested for compressive strength and tensile strength in bending. Also, 15 concrete cube samples were tested for compressive strength, 15 concrete prism samples for axial compressive strength, 15 concrete prism specimens for tensile strength in bending, and 15 concrete prism samples for axial tensile strength; in total—45 prism specimens were tested.

For the manufacture of prototypes of cement and concrete mixtures, technological equipment, testing equipment and measuring instruments were used as in [31,54,57–61].

A detailed description of the methods for determining the strength and deformation characteristics of prototype concrete samples is presented in [51]. The compressive strength and tensile strength in bending of the hardened cement paste samples were determined according to the GOST 30744 method “Methods of testing with using polyfraction standard sand” [62]. The compressive strength, flexural tensile strength and axial tensile strength of concrete were determined according to GOST 10180 “Concretes. Methods for strength determination using reference specimens” [63], and axial compressive strength of concrete

according to GOST 24452 “Concretes. Methods of prismatic, compressive strength, modulus of elasticity and Poisson’s ratio determination” [64].

The study of the microstructure of “the modified hardened cement paste was carried out using a ZEISS CrossBeam 340 (Carl Zeiss Microscopy GmbH (Factory), Jena, Germany)” [51]. Also, chemical analysis was carried out using this two-beam scanning electron/ion microscope, equipped with an Oxford Instruments X-Max 80 X-ray microanalyzer [51].

3. Results and Discussion

After 28 days of hardening, laboratory tests of the experimental compositions of cement pastes and concrete mixtures were carried out for strength and deformation characteristics. Photographs of samples of hardened cement pastes subjected to electromagnetic treatment and containing rice straw biochar are shown in Figure 5.

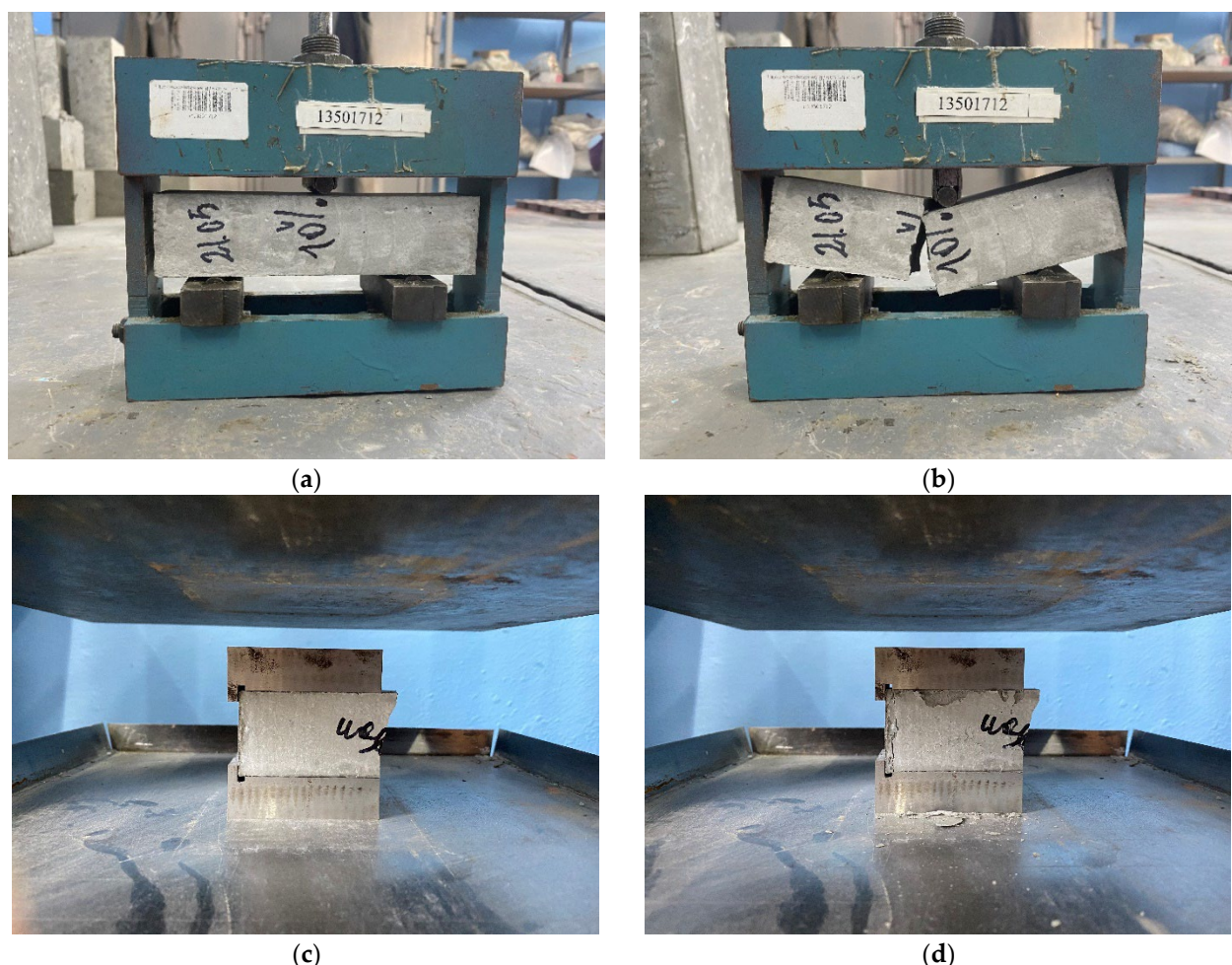


Figure 5. Samples of hardened cement paste modified with RSA and activated by electromagnetic treatment in a bending test: (a) to failure; (b) after failure and in compression test: (c) before failure; (d) after destruction.

Table 7 presents the strength properties of cement mixtures.

The best results in terms of compressive and tensile strength in bending were shown by samples of the hardened cement paste processed in the UAP and containing 5% RSA: the increase in strength compared to the control samples was 22%. A slightly smaller increase (18%) was shown by the samples processed in the UAP, but without RSA. In compositions with dosages of 10% and 15% RSA, a drop in strength up to 30% was observed.

Table 7. The strength properties of cement mixtures.

Composition Number	Compressive Strength, MPa	Tensile Strength in Bending, MPa
1	40.8 ± 2.4	5.82 ± 0.36
2	47.9 ± 2.7	6.41 ± 0.33
3	49.5 ± 2.5	7.09 ± 0.34
4	38.4 ± 2.4	5.71 ± 0.38
5	28.5 ± 1.7	5.02 ± 0.36

Electromagnetic treatment of cement mixtures allows a modified particle surface structure to be obtained, which leads to an intensification of the process of mixing concrete with water. The combined effect of electromagnetic treatment of the cement mixture and rice straw biochar nanomodification optimizes the curing cycle of cement composites by reducing the curing time and leads to structure strengthening [54].

The strength properties of the compositions of concrete are presented in Figures 6–9.

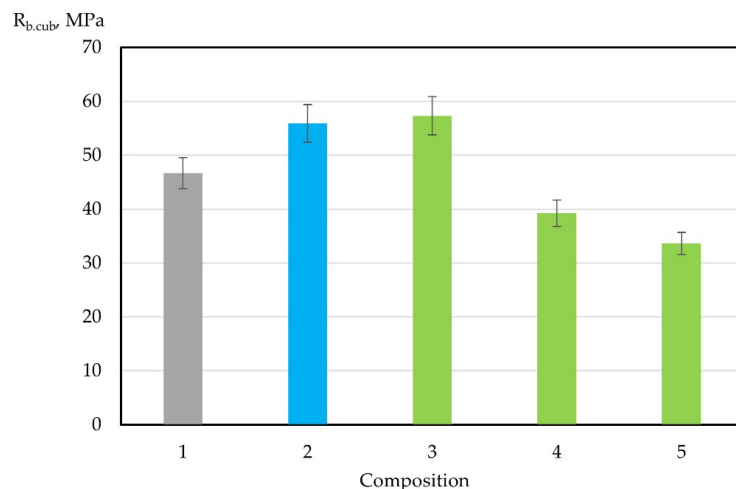


Figure 6. Change in compressive strength of concrete samples at the age of 28 days: 1 (grey)—control composition; 2 (blue)—electromagnetically treated cement paste without RSA; 3, 4, 5 (green)—electromagnetic treated cement paste with RSA of different dosage according to Table 6.

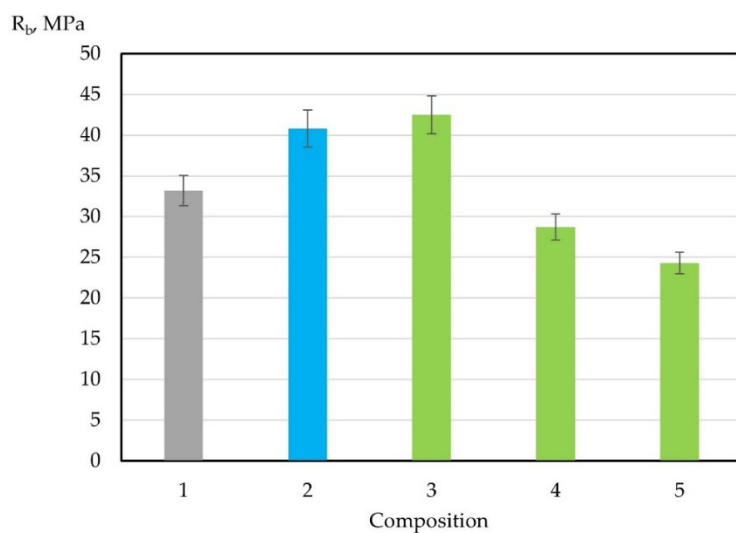


Figure 7. Change in axial compressive strength of concrete samples at the age of 28 days: 1 (grey)—control composition; 2 (blue)—electromagnetically treated cement paste without RSA; 3, 4, 5 (green)—electromagnetic treated cement paste with RSA of different dosage according to Table 6.

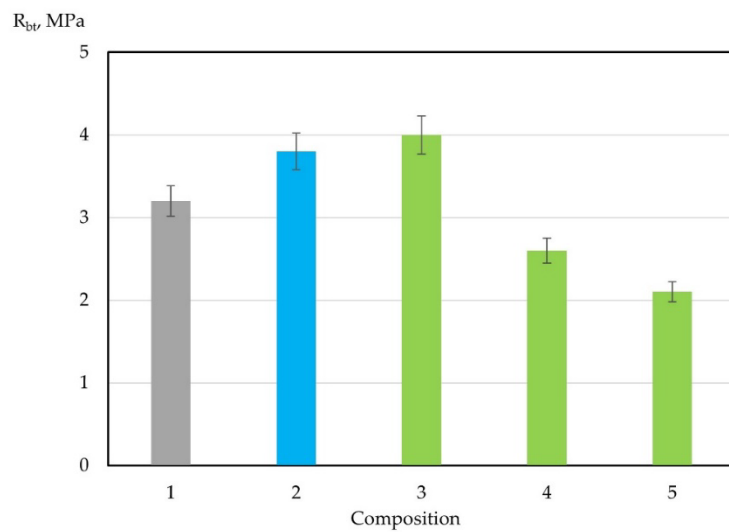


Figure 8. Change in axial tensile strength of concrete samples at the age of 28 days: 1 (grey)—control composition; 2 (blue)—electromagnetically treated cement paste without RSA; 3, 4, 5 (green)—electromagnetic treated cement paste with RSA of different dosage according to Table 6.

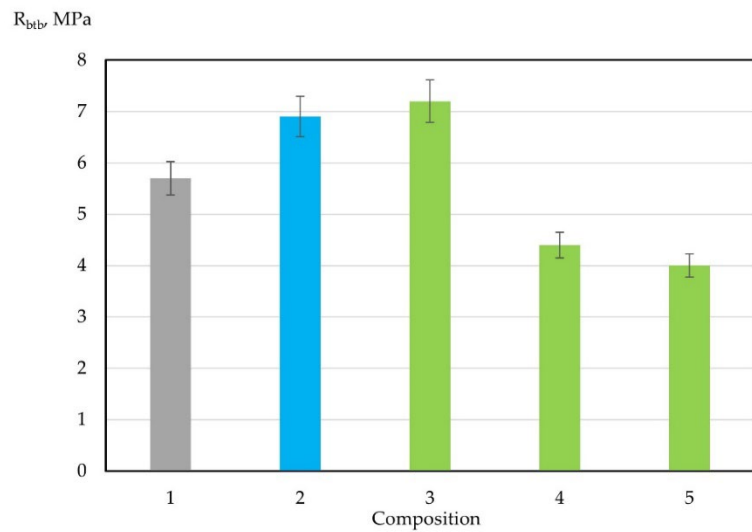


Figure 9. Change in tensile strength in bending of concrete samples at the age of 28 days: 1 (grey)—control composition; 2 (blue)—electromagnetically treated cement paste without RSA; 3, 4, 5 (green)—electromagnetic treated cement paste with RSA of different dosage according to Table 6.

According to the results of determining the compressive strength, it was found that the maximum values were recorded for concrete samples made on activated cement paste with 5% RSA, and the minimum values were for samples of composition No. 5, made on activated concrete mix with 15% RSA. Thus, the increase in the strength of composition No. 2 in comparison with the control was 20%, and the increase in the strength of composition No. 3 was 23%. As for compositions No. 4 and No. 5, there was a drop in strength characteristics by 16% and 28%, respectively.

The change in axial compressive strength, axial tension, and bending tensile strength had a similar behavior as the change in compressive strength. Thus, the increase in the axial compressive strength of compositions No. 2 and 3 was 23% and 28% percent, respectively, and, for compositions No. 4 and 5, a drop in strength by 14% and 27% was noted. The increases in axial compressive and flexural tensile strengths of compositions Nos. 2 and 3 were 19% and 25% for axial compressive strength and 21% and 26% for flexural tensile strength. The strength drops of compositions No. 2 and 3 were 19% and 34% for the axial compressive strength and 23% and 30% for the tensile strength in bending.

The results of the strain properties of concrete are presented in Figures 10 and 11.

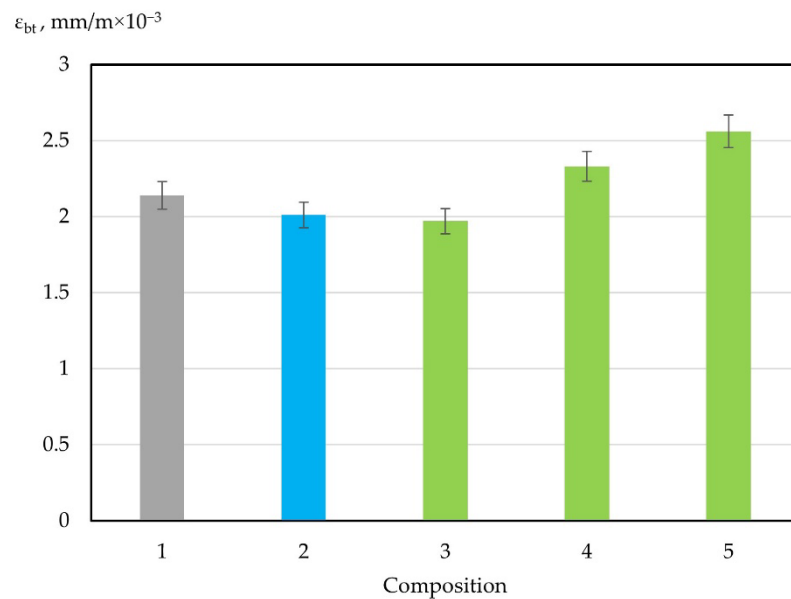


Figure 10. Change in ultimate strains under axial compression of concrete samples at the age of 28 days: 1 (grey)—control composition; 2 (blue)—electromagnetically treated cement paste without RSA; 3, 4, 5 (green)—electromagnetic treated cement paste with RSA of different dosage according to Table 6.

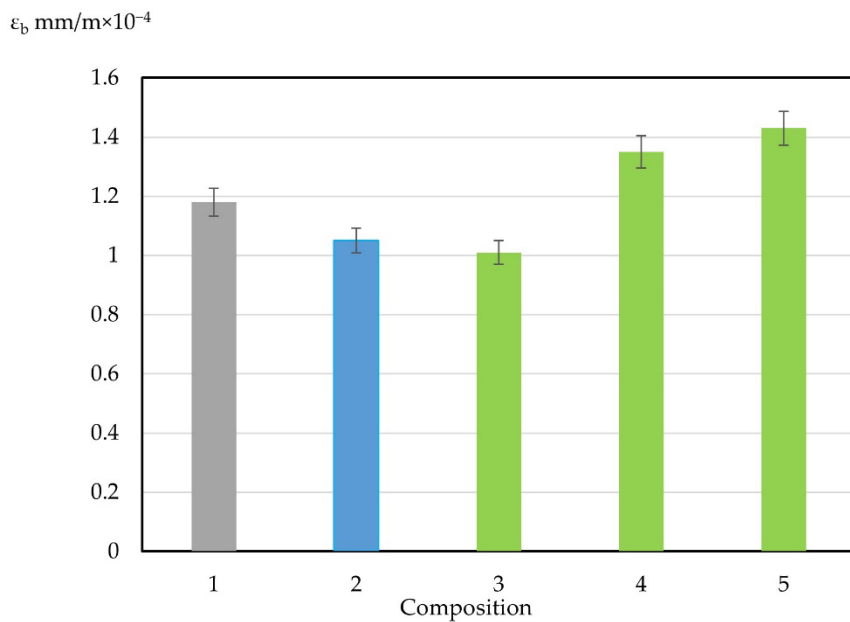


Figure 11. Change in ultimate strains during axial tension of concrete samples at the age of 28 days: 1 (grey)—control composition; 2 (blue)—electromagnetically treated cement paste without RSA; 3, 4, 5 (green)—electromagnetic treated cement paste with RSA of different dosage according to Table 6.

Figures 10 and 11 show that the values of ultimate strains under axial compression and tension of the experimental compositions No. 2 and 3 decreased in comparison with the values of the control composition, while for compositions No. 4 and 5, they increased. Deformations under axial compression of composition No. 2 decreased by 6%, and of composition No. 3 by 8%. For compositions No. 4 and 5, these deformations increased by 9% and 20%, respectively. As for the deformations during axial tension, for compositions

No. 2 and 3, their values decreased by 11% and 14%, respectively, and for compositions No. 4 and 5, they increased by 14% and 21% compared with the control composition. Such changes in deformations are explained by sacrifices in the strength characteristics of the compositions, recorded above (Figures 6–9).

The nanomodifier introduced in the optimal amount becomes the center of crystallization of the emerging concrete microstructure. In this case, the structure has the densest packing of particles and, accordingly, the best mechanical and deformation characteristics. A powerful rotating electromagnetic field is created inside the UAP, which rotates ferromagnetic elements—needles, which, due to a powerful electromagnetic field and their ferromagnetic properties, interact with the main rotating field, thus creating their own local fields. As a result, during activation, a number of effects occur in the UAP, in particular, magnetostrictive and cavitation effects, which strongly affect the change in the properties of the processed materials [54].

The authors note a significant decrease in the strength of compositions 4 and 5, the possible cause and mechanism of which can be explained by the following fact. As is known from the previously published work [54], excessive saturation of a building composite with a nanomodifier can lead to negative consequences. Thus, the formation of the structure at the micro- and macrolevels is threatened in the sense that there is no denser packing of particles and proper lubrication with the cement matrix of the filler, which is the modifier. As a result, the processes of hydration and structure formation become more difficult. Such events lead to the fact that, when the structure deteriorates, it is logical that the strength characteristics also decrease. Two main conclusions can be drawn from this. It is important to observe a rational dosage of the nanomodifier in order to simultaneously achieve the maximum effect from it and, at the same time, allow certain intervals so that the strength characteristics do not subsequently decrease. The presence of additional electromagnetic treatment during the nanomodification of concrete with rice straw biochar somewhat slows down the destructive processes; that is, the formation of the structure is somewhat improved compared to the same process when non-activated concrete is supersaturated, but still, due to the fundamental processes occurring in this case, it is impossible to stop them. That is why the need to achieve the optimal dosage of the components is once again emphasized.

Figures 12 and 13 show compression diagrams “ ε_b - σ_b ” and tension “ ε_{bt} - σ_{bt} ” for all experimental compositions.

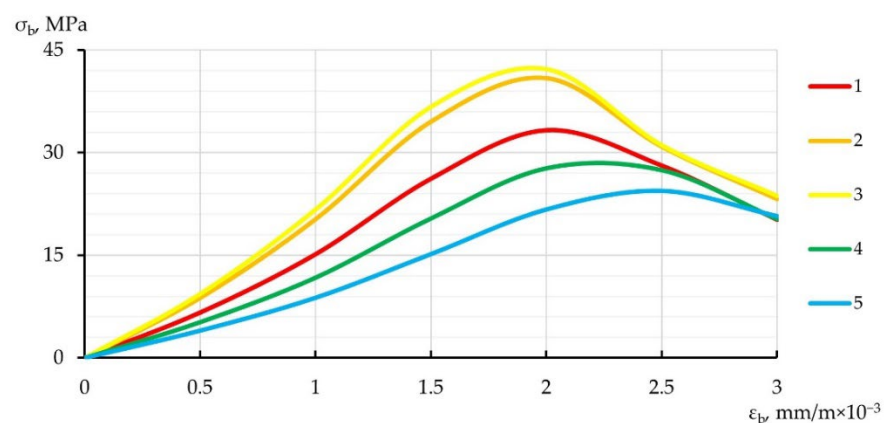


Figure 12. Stress-strain diagram in compression.

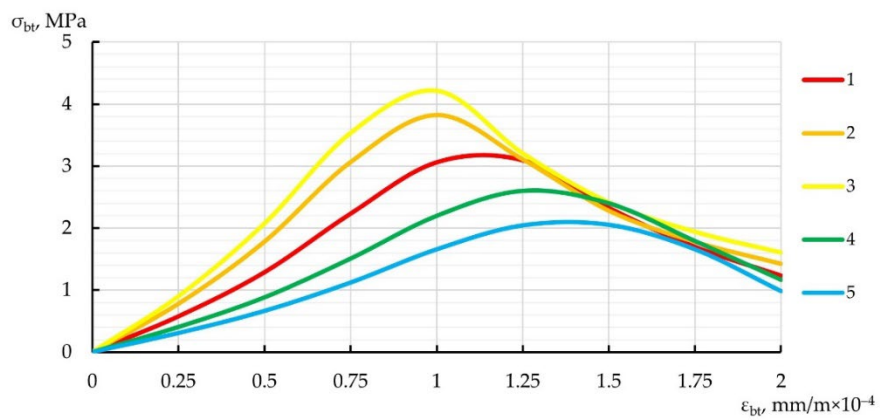


Figure 13. Tensile stress-strain diagram.

Figures 12 and 13 show that the peak of the “stress-strain” diagrams of the most effective compositions No. 2 and 3, previously established according to the strength characteristics of concrete, is shifted up and to the left relative to the concretes of the control composition No. 1 and compositions No. 4 and 5. Shift of the peak of the diagrams compression and tension indicates an increase in strength characteristics and a better resistance of such concrete to deformations, thereby confirming the hypothesis of an increase in strength characteristics and a better resistance of such concrete to deformations due to electromagnetic treatment and nanomodification of rice straw with biochar in an amount of 5% instead of a part of cement.

Figures 14–18 show SEM images of the structure of hardened cement mixes for all five experimental formulations.

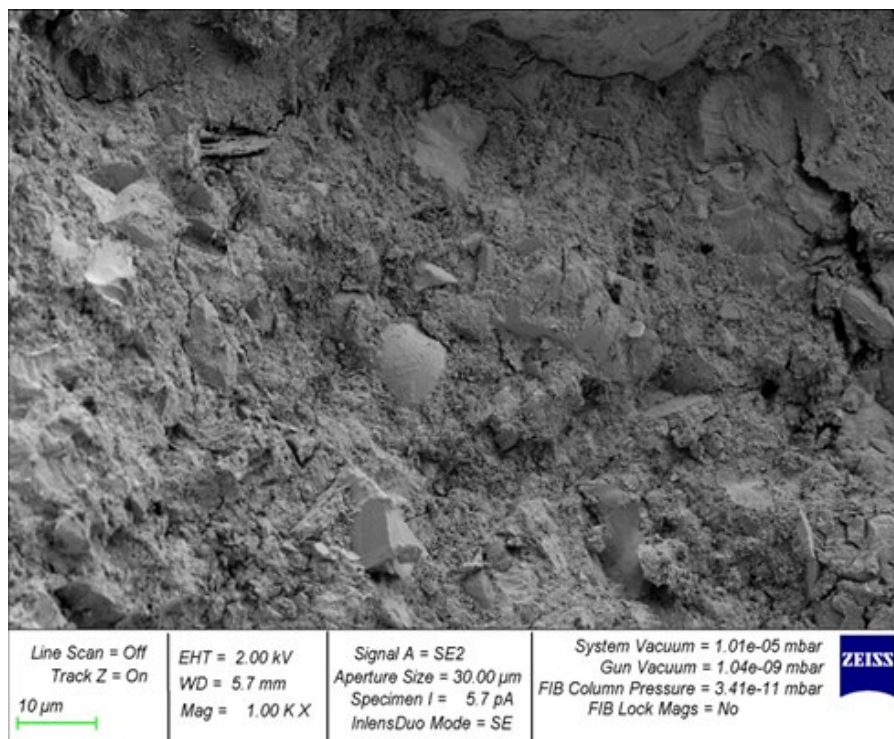


Figure 14. SEM image of the structure of the hardened cement paste of the control composition.

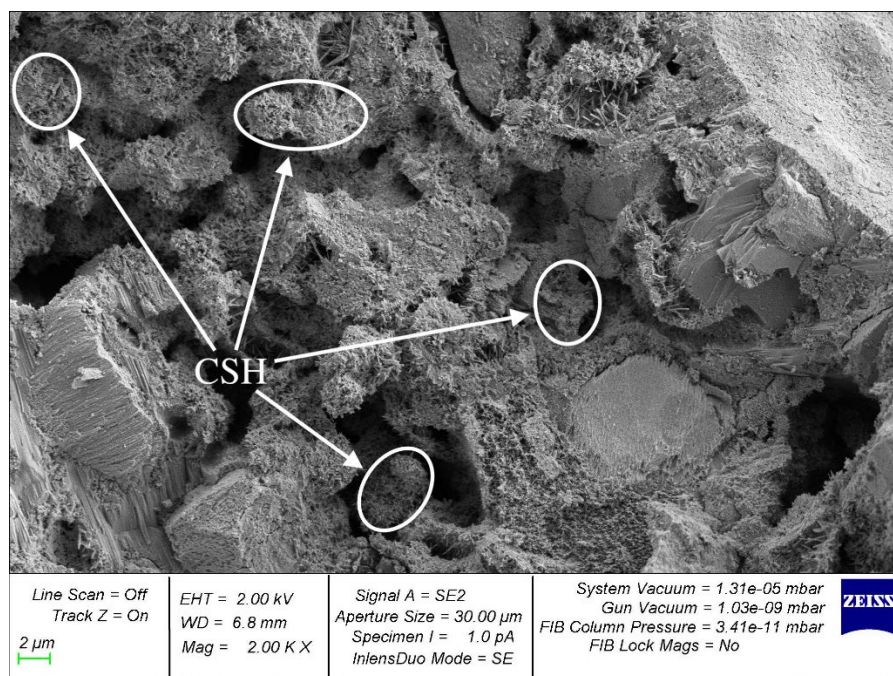


Figure 15. SEM image of the structure of a hardened cement paste subjected to electromagnetic processing.

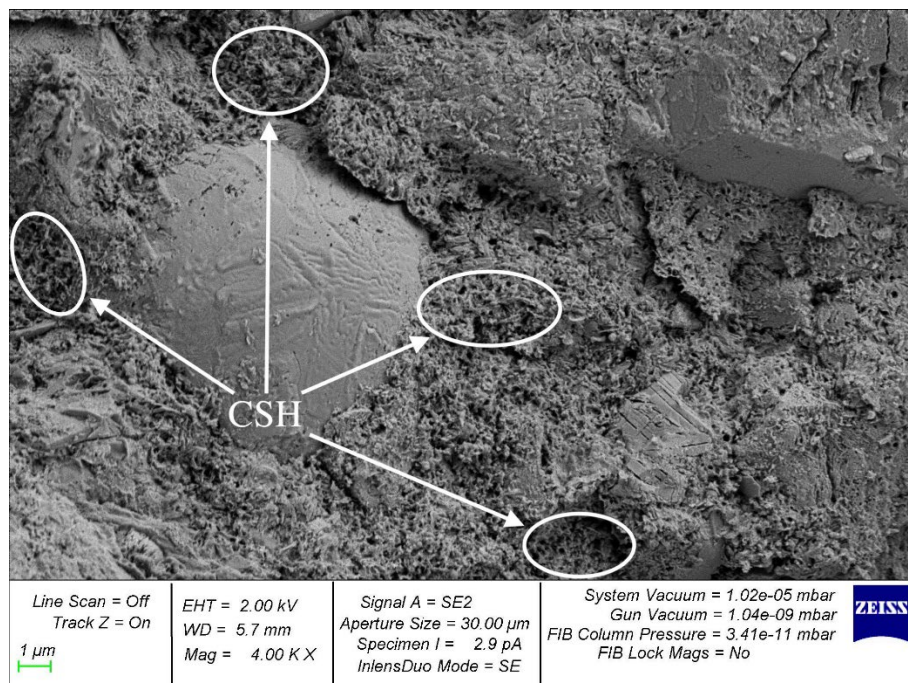


Figure 16. SEM image of the structure of an electromagnetically treated hardened cement paste with 5% RSA in place of part of the cement.

The SEM image data shows a clear spread of the calcium silicate hydrate (CSH) gel. Figure 14 shows the structure of the hardened cement paste of the control composition. As can be seen, it consists of irregularly shaped particles with micropores; cracking is also observed. Figures 15 and 16 show, respectively, the structure of the hardened cement paste subjected to electromagnetic processing and the structure of the cement paste processed in UAP with 5 wt.% RSA. The structure of these cement compositions is denser and more homogeneous, which is explained by a large amount of CSH. This may be the reason for

some increase in the strength characteristics of compositions Nos. 2 and 3. As the RSA content in compositions Nos. 4 and 5 increases, the structure of the cement stone becomes less dense and has a loose character, and CSH gel is not observed everywhere, which is the reason for the sharp drop in strength characteristics (Figures 17 and 18). Thus, the analysis of the microstructure of all the studied compositions is in good agreement with the above results of the strength and deformation properties of the studied concretes and confirms the high efficiency of electromagnetic treatment and nanomodification of rice straw biochar of cement composites.

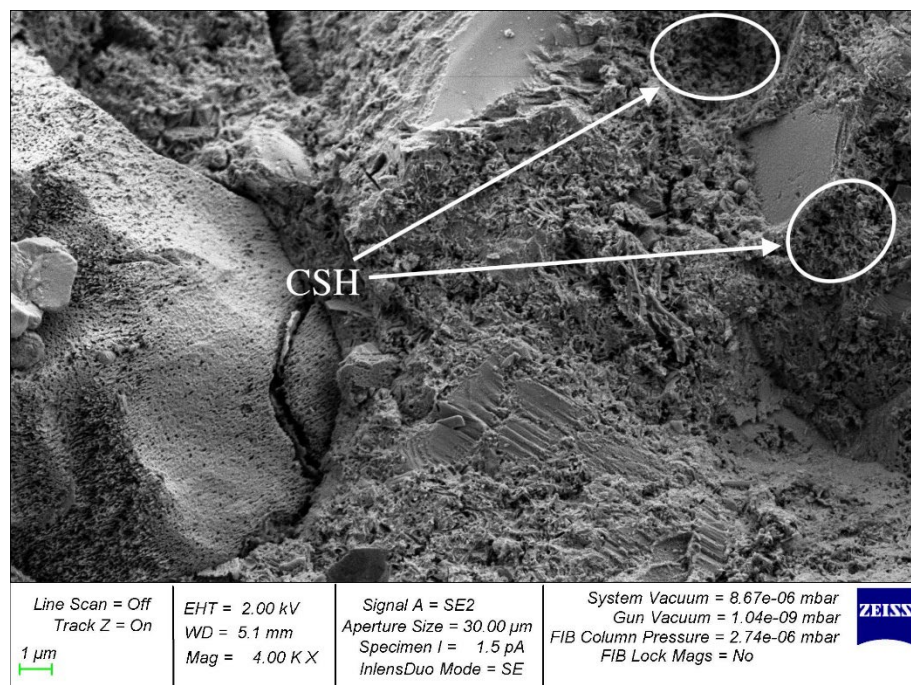


Figure 17. SEM image of the structure of an electromagnetically treated hardened cement paste with 10% RSA in place of part of the cement.

To discuss the results obtained, let us now consider the fundamental foundations of the physicochemical processes occurring during the electromagnetic activation of nanomodifiers for the resulting concrete. Based on the known data [65,66], we present our interpretation of these processes. Let us derive a mathematical model of the above-mentioned fundamental processes.

The process of mechanical activation of materials in UAP, as in other mixers, is usually described by several stages [65,66]. At the first stage, electromagnetic processing causes a violation of the crystal lattice of the material and changes in interplanar distances and orientation angles of the structure. At the second stage, a new surface of the system is formed, cracks appear and develop in the material. In this case, the growth of the total energy of the system with an increase in the phase interface by 1 cm^2 is determined by the formula:

$$\Delta H_s = \sigma - T \frac{d\sigma}{dT} = \sigma + q \quad (1)$$

where σ is the specific surface energy; T is temperature; and q is the latent heat of formation of 1 cm^3 of a new surface.

The mechanism of the effect of magnetostriction on a substance is simple: any particle of any material, being in contact with the needle at the moment of magnetization reversal, experiences a powerful blow, since the change in polarity occurs in a very short time, comparable to the speed of light, taking into account, of course, losses for the time of displacement or rotation of domain boundaries.

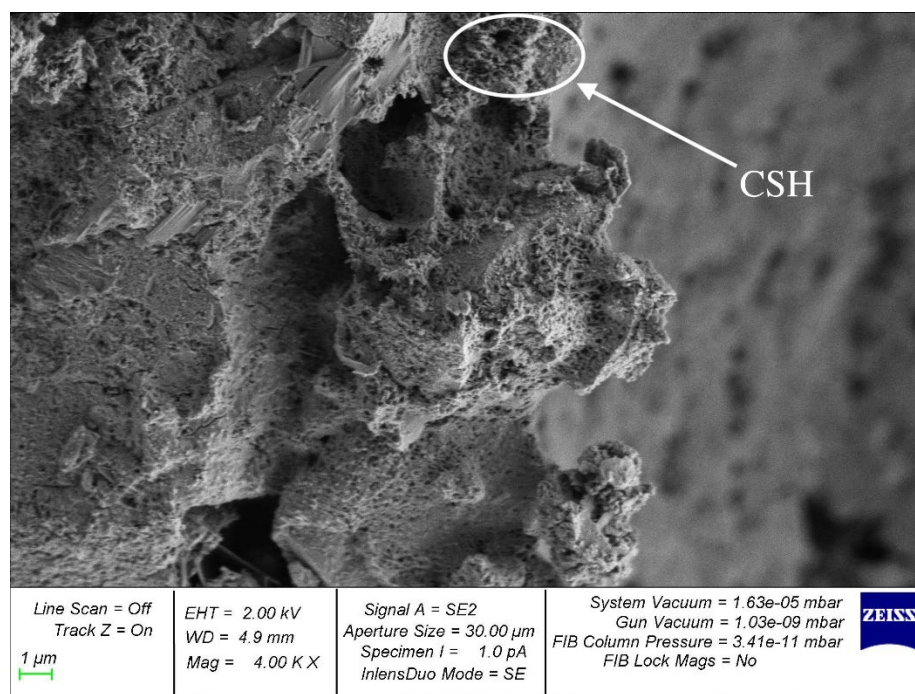


Figure 18. SEM image of the structure of an electromagnetically treated hardened cement paste with 15% RSA in place of part of the cement.

Studies [65,66] show that a nonmagnetic particle can move in a vortex layer even in the direction opposite to the direction of its transportation through the vortex layer. For example, a freely falling particle in contact with a moving ferromagnetic element can acquire a speed opposite to the speed before the collision, and, as it were, is reflected from the vortex layer. Similar phenomena are also observed inside the vortex layer. As a result, the duration of stay of a non-magnetic particle in the vortex layer significantly exceeds the time during which it flies a distance equal to the length of the vortex layer.

Thus, when mixing in a vortex layer, ferromagnetic elements can be considered as parallel “elementary” layers (Figure 19).

Let's determine the area S_4 of the “dead” zone, for which we select $(\sqrt{n_1 - 1})^2$ squares with sides $(l + x)$ inside the section under consideration. Area S_5 is in the “dead” zone

$$S_5 = (l + x)^2 - \frac{\pi D^2}{4} \quad (2)$$

The “dead” zone includes two more types of regions S_6, S_7 the number of which is, respectively, equal to $4(\sqrt{n_1} - 1)$ and 4, and the areas of these zones:

$$S_6 = \left(l + x \frac{l}{2} \right) \quad (3)$$

$$S_7 = \frac{l^2}{4} - \frac{\pi l^2}{16} \quad (4)$$

The total area of the “dead” zone in the section:

$$S_D = (\sqrt{n_1} - 1)S_6 + 4(\sqrt{n_1} - 1)S_7 + 4S_8 \quad (5)$$

This expression reflects the area deduced by the authors [65,66] where activation is impossible because of ongoing processes and the action of rotational forces. That is, this is the minimum error of the method, expressed quantitatively in units of area.

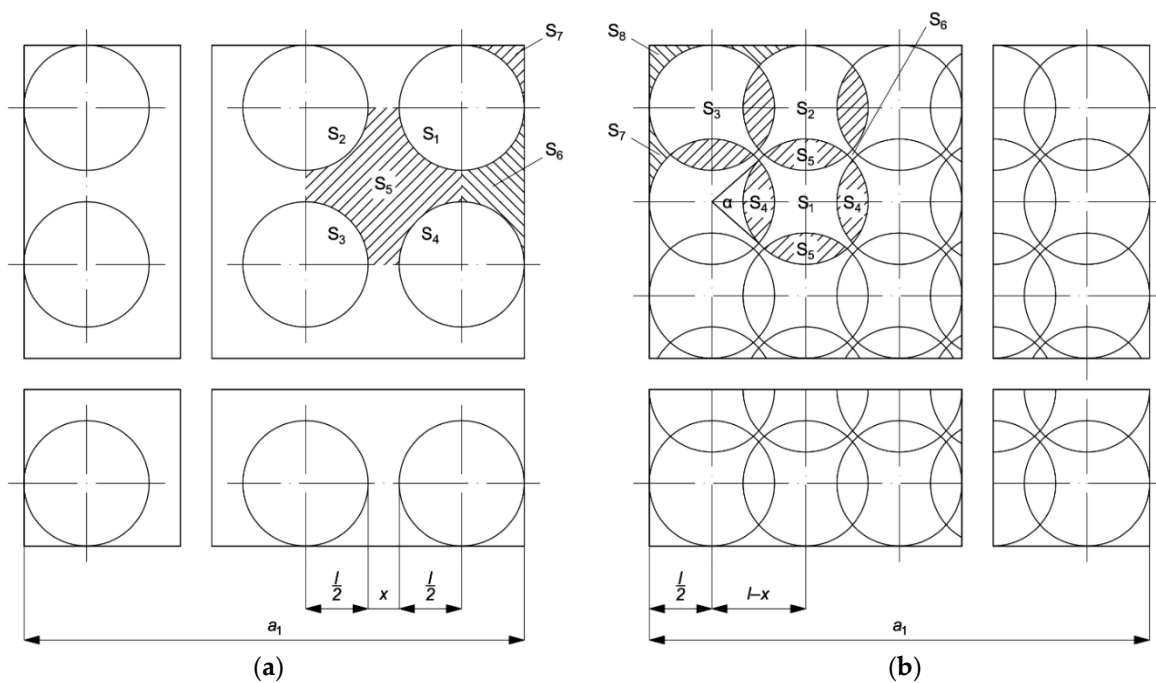


Figure 19. Models of the mixing process in a vortex layer: (a) the case when the zones of rotation of ferromagnetic elements do not intersect; (b) the case when the rotation zones of ferromagnetic elements intersect.

The graphical models of the fundamental processes of electromagnetic activation of nanomodifiers for concrete presented by us have been verified according to the theoretical data obtained earlier by the authors [65,66] and the results of our own experimental verification. Thus, we have described the mechanism and physical and chemical essence of improving the micro- and macrostructure and properties of concretes of a new type.

In addition, the efficiency of electromagnetic treatment of cement paste with rice straw biochar of the selected optimal dosage has been theoretically and experimentally confirmed. In contrast to [54], where only rice straw biochar was subjected to electromagnetic treatment, in this study, a mixture of cement with biochar and water was already activated. At the same time, the efficiency of electromagnetic treatment of the mixture is up to 10% higher than that of biochar alone, which is confirmed by the test results obtained for strength and deformation parameters in comparison with [54].

4. Conclusions

The conducted experimental studies and analysis led to the following conclusions:

- (1) The results of the joint influence of electromagnetic activation and nanomodification by rice straw biochar on the strength and deformation characteristics of concrete were experimentally verified and confirmed by microstructure analysis;
- (2) Electromagnetic treatment of the cement paste increased the compressive strength, axial compressive strength, tensile strength in bending, and axial tensile strength of concrete. The best performance was demonstrated by electromagnetically activated concrete containing 5 wt.% rice straw biochar. Strength characteristics increased from 23% to 28% depending on the type of strength, and deformations decreased from 8% to 14% in comparison with the control concrete composition. Replacing part of the cement with 10 wt.% and 15 wt.% biochar from rice straw led to a strong drop in strength characteristics from 14 to 34% and an increase in deformation characteristics from 9 to 21%;
- (3) The conducted microstructural studies prove the positive effect of electromagnetic treatment on the structure of the cement composite both with and without the addition

of rice straw biochar. Improving the structure at the micro- and macrolevels is due to the creation of additional centers of crystallization, denser packing of particles, and a decrease in defectiveness at the phase boundaries due to the optimal nanomodification of concrete with activated finely dispersed rice straw biochar.

The use of concretes containing RSA waste and activated by electromagnetic treatment is promising in real construction practice. The use of waste rice straw charcoal as a partial replacement for cement solves two particularly important problems at once: environmental, the utilization of agricultural waste, and economic, the reduction of the cost of construction by reducing the consumption of one of the most expensive components—cement.

Author Contributions: Conceptualization, S.A.S., E.M.S., A.N.B. and N.D.; methodology, A.S.S., S.A.S., E.M.S. and V.V.; software, S.A.S., E.M.S., A.N.B. and N.B.; validation, N.D., S.A.S., E.M.S. and A.N.B.; formal analysis, N.D., S.A.S. and E.M.S.; investigation, A.S.S., N.B., L.R.M., S.A.S., E.M.S., A.N.B. and B.M.; resources, B.M.; data curation, S.A.S., E.M.S. and N.D.; writing—original draft preparation, S.A.S., E.M.S. and A.N.B.; writing—review and editing, S.A.S., E.M.S. and A.N.B.; visualization, S.A.S., E.M.S., A.N.B., V.V. and N.B.; supervision, L.R.M. and B.M.; project administration, L.R.M. and B.M.; funding acquisition, A.N.B. and B.M. All authors have read and agreed to the published version of the manuscript.

Funding: This research received no external funding.

Institutional Review Board Statement: Not applicable.

Informed Consent Statement: Not applicable.

Data Availability Statement: The study did not report any data.

Acknowledgments: The authors would like to acknowledge the administration of Don State Technical University for their resources and financial support.

Conflicts of Interest: The authors declare no conflict of interest.

References

- Doan, D.T.; Ghaffarianhoseini, A.; Naismith, N.; Zhang, T.; Ghaffarianhoseini, A.; Tookey, J. A critical comparison of green building rating systems. *Build. Environ.* **2017**, *123*, 243–260. [[CrossRef](#)]
- Hwang, B.-G.; Zhu, L.; Tan, J.S.H. Green business park project management: Barriers and solutions for sustainable development. *J. Clean. Prod.* **2017**, *153*, 209–219. [[CrossRef](#)]
- Tang, Z.; Li, W.; Tam, V.W.Y.; Xue, C. Advanced progress in recycling municipal and construction solid wastes for manufacturing sustainable construction materials. *Resour. Conserv. Recycl. X* **2020**, *6*, 100036. [[CrossRef](#)]
- Miller, S.A. Supplementary cementitious materials to mitigate greenhouse gas emissions from concrete: Can there be too much of a good thing? *J. Clean. Prod.* **2018**, *178*, 587–598. [[CrossRef](#)]
- Habert, G.; Miller, S.A.; John, V.M.; Provis, J.L.; Favier, A.; Horvath, A.; Scrivener, K.L. Environmental impacts and decarbonization strategies in the cement and concrete industries. *Nat. Rev. Earth Environ.* **2020**, *1*, 559–573. [[CrossRef](#)]
- Li, X.; Qin, D.; Hu, Y.; Ahmad, W.; Ahmad, A.; Aslam, F.; Joyklad, P. A systematic review of waste materials in cement-based composites for construction applications. *J. Build. Eng.* **2022**, *45*, 103447. [[CrossRef](#)]
- Bueno, E.T.; Paris, J.M.; Clavier, K.A.; Spreadbury, C.; Ferraro, C.C.; Townsend, T.G. A review of ground waste glass as a supplementary cementitious material: A focus on alkali-silica reaction. *J. Clean. Prod.* **2020**, *257*, 120180. [[CrossRef](#)]
- Sood, D.; Hossain, K.M.A. Strength, Shrinkage and Early Age Characteristics of One-Part Alkali-Activated Binders with High-Calcium Industrial Wastes, Solid Reagents and Fibers. *J. Compos. Sci.* **2021**, *5*, 315. [[CrossRef](#)]
- Sood, D.; Hossain, K.M.A. Optimizing Precursors and Reagents for the Development of Alkali-Activated Binders in Ambient Curing Conditions. *J. Compos. Sci.* **2021**, *5*, 59. [[CrossRef](#)]
- Camara, L.A.; Wons, M.; Esteves, I.C.A.; Medeiros-Junior, R.A. Monitoring the Self-healing of Concrete from the Ultrasonic Pulse Velocity. *J. Compos. Sci.* **2019**, *3*, 16. [[CrossRef](#)]
- Boakye, K.; Khorami, M.; Saidani, M.; Ganjian, E.; Dunster, A.; Ehsani, A.; Tyrer, M. Mechanochemical Characterisation of Calcined Impure Kaolinitic Clay as a Composite Binder in Cementitious Mortars. *J. Compos. Sci.* **2022**, *6*, 134. [[CrossRef](#)]
- Luhar, S.; Luhar, I.; Shaikh, F.U.A. A Review on the Performance Evaluation of Autonomous Self-Healing Bacterial Concrete: Mechanisms, Strength, Durability, and Microstructural Properties. *J. Compos. Sci.* **2022**, *6*, 23. [[CrossRef](#)]
- Wang, H.; Mustaffar, A.; Phan, A.N.; Zivkovic, V.; Reay, D.; Law, R.; Boodhoo, K. A review of process intensification applied to solids handling. *Chem. Eng. Process. Process. Intensif.* **2017**, *118*, 78–107. [[CrossRef](#)]
- Bhatty, J.I.; Miller, F.M.; Boahn, R.P. *Innovations in Portland Cement Manufacturing*, 2nd ed.; Portland Cement Association: Skokie, IL, USA, 2004; p. 1734.

15. Genç, Ö. Energy-Efficient Technologies in Cement Grinding. High. Performance Concrete Technology and Applications. 2016. Available online: <https://doi.org/10.5772/64427> (accessed on 5 August 2022). [CrossRef]
16. Frances, C.; Le Bolay, N.; Belaroui, K.; Pons, M.N. Particle morphology of ground gibbsite in different grinding environments. *Int. J. Miner. Process.* **2001**, *61*, 41–56. [CrossRef]
17. Bond, F.C. Control Particle Shape and Size. *Chem. Eng. Aug.* **1954**, *61*, 195–198.
18. Holt, C.B. The Shape of Particles Produced by Comminution, A Review. *Powder Technol.* **1981**, *28*, 59–63. [CrossRef]
19. Durney, T.E.; Meloy, T.P. Particle Shape Effects due to Crushing Method and Size. *Int. J. Miner. Process.* **1986**, *16*, 109–123. [CrossRef]
20. Kaya, E.; Hogg, R.; Kumar, S.R. Particle Shape Modification in Comminution. *KONA Powder Part. J.* **2002**, *20*, 188–195. [CrossRef]
21. Dumm, T.F.; Hogg, R. Characterization of Particle Shape. In Proceedings of the International Symposium on Respirable Dust in the Mineral Industries, Pittsburgh, PA, USA; SME: Littleton, CO, USA, 1990; pp. 283–288.
22. Panigrahy, P.K.; Medhe, M.; Sahu, R.M.; Pandey, S.P.; Chatterjee, A.K. Quantitative morphological Characterization of Cement Particles of Different Milling Systems and Its Relationship with Physical Properties of Cements. Available online: <https://en.jcement.ru/magazine/329/10177/> (accessed on 5 August 2022).
23. Gailitis, R.; Figiela, B.; Abelkalns, K.; Sprince, A.; Sahmenko, G.; Choinska, M.; Guigou, M.D. Creep and Shrinkage Behaviour of Disintegrated and Non-Disintegrated Cement Mortar. *Materials* **2021**, *14*, 7510. [CrossRef]
24. Marzouki, A.; Lecomte, A.; Beddey, A.; Diliberto, C.; Ouezdou, M.B. The effects of grinding on the properties of Portland-limestone cement. *Constr. Build. Mater.* **2013**, *48*, 1145–1155. [CrossRef]
25. Pacana, A.; Siwiec, D.; Bednarova, L.; Sofranko, M.; Vegsoova, O.; Cvoliga, M. Influence of Natural Aggregate Crushing Process on Crushing Strength Index. *Sustainability* **2021**, *13*, 8353. [CrossRef]
26. Tole, I.; Habermehl-Cwirzen, K.; Cwirzen, A. Optimization of the Process Parameters Controlling the Degree of Amorphization during Mechanical Activation of Clay Using the Taguchi Method. In Proceedings of the 1st International Conference on Smart Materials for Sustainable Construction (SMASCO 2019), Luleå, Sweden, 10–12 December 2019. [CrossRef]
27. Ostrowski, K.A.; Kinasz, R.; Dybel, P. The Impact of Surface Preparation for Self-Compacting, High-Performance, Fiber-Reinforced Concrete Confined with CFRP Using a Cement Matrix. *Materials* **2020**, *13*, 2830. [CrossRef] [PubMed]
28. Soares, S.; Sena-Cruz, J.; Cruz, J.R.; Fernandes, P. Influence of Surface Preparation Method on the Bond Behavior of Externally Bonded CFRP Reinforcements in Concrete. *Materials* **2019**, *12*, 414. [CrossRef] [PubMed]
29. Khan, K.; Ishfaq, M.; Amin, M.N.; Shahzada, K.; Wahab, N.; Faraz, M.I. Evaluation of Mechanical and Microstructural Properties and Global Warming Potential of Green Concrete with Wheat Straw Ash and Silica Fume. *Materials* **2022**, *15*, 3177. [CrossRef]
30. Ibragimov, R.A.; Korolev, E.V.; Deberdeev, T.R.; Leksin, V.V. Durability of heavy-weight concrete with portland cement treated in apparatus of vortex layer. *Constr. Mater.* **2017**, *10*, 28–31. [CrossRef]
31. Shcherban', E.M.; Stel'makh, S.A.; Beskopylny, A.; Mailyan, L.R.; Meskhi, B.; Shuyskiy, A. Improvement of Strength and Strain Characteristics of Lightweight Fiber Concrete by Electromagnetic Activation in a Vortex Layer Apparatus. *Appl. Sci.* **2022**, *12*, 104. [CrossRef]
32. Adoshev, A.; Antonov, S.; Yastrebov, S.; Melnikov, M. Ferro-vortex apparatus. *Eng. Rural. Dev.* **2017**, *1*, 804–810. [CrossRef]
33. Sekulic, Z.; Popov, S.; Đurić, M.; Rosić, A. Mechanical activation of cement with addition of fly ash. *Mater. Lett.* **1999**, *39*, 115–121. [CrossRef]
34. Sayer, S.M.; Dahlin, A. Propagation of ultrasound through hydrating cement parts at early times. *Adv. Cem. Based Mater.* **1993**, *1*, 12–21. [CrossRef]
35. Kennedy, D.P. *A Study to Determine and Quantify the Benefits of Using Power Ultrasound Technology in a Precast Concrete Manufacturing Environment*; Trinity College: Dublin, Ireland, 2012; pp. 184–191.
36. Intini, G.; Liberti, L.; Notarnicola, M.; Di Canio, F. Mechanochemical activation of coal fly ash for production of high strength cement conglomerates. *Chem. Sustain. Dev.* **2009**, *17*, 567–571. Available online: https://www.sibran.ru/upload/iblock/411/mechanochemical_activation_of_coal_fly_ash_for_production_of_high_strength_cement_conglomerates.pdf (accessed on 5 August 2022).
37. Sprince, A.; Pakrastins, L.; Baskers, B.; Gaile, L. Crack development research in extra fine aggregate cement composites. *Proc. Int. Sci. Pract. Conf.* **2015**, *1*, 205–208. [CrossRef]
38. Ibragimov, R.; Korolev, E.; Kayumov, R.A.; Deberdeev, R.; Leksin, V.V.; Sprince, A. Efficiency of activation of mineral binders in vortex-layer devices. *Mag. Civ. Eng.* **2018**, *82*, 191–198. [CrossRef]
39. Al-Maliki, A.A.K.; Aswed, K.K.; Abraheem, A.K. Properties of concrete with magnetic mixing water. *AIP Conf. Proc.* **2020**, *2213*, 020146. [CrossRef]
40. Isam, T.; Abdel-Magid, M.; Hamdan, R.M.; Abdelgader, A.A.B.; Omer, M.E.A.; Ahmed, N.M.R.-A. Effect of Magnetized Water on Workability and Compressive Strength of Concrete. *Procedia Eng.* **2017**, *193*, 494–500. [CrossRef]
41. Milton, J.C.; Gnanaraj, P.A. Compressive Strength of Concrete with Nano Cement. In *Cement Industry: Optimization, Characterization and Sustainable Application*; IntechOpen: London, UK, 2021. [CrossRef]
42. Malathy, R.; Shanmugam, R.; Chung, I.-M.; Kim, S.-H.; Prabakaran, M. Mechanical and Microstructural Properties of Composite Mortars with Lime, Silica Fume and Rice Husk Ash. *Processes* **2022**, *10*, 1424. [CrossRef]
43. Sobuz, M.H.R.; Saha, A.; Anamika, J.F.; Houda, M.; Azab, M.; Akid, A.S.M.; Rana, M.J. Development of Self-Compacting Concrete Incorporating Rice Husk Ash with Waste Galvanized Copper Wire Fiber. *Buildings* **2022**, *12*, 1024. [CrossRef]

44. Safari, J.; Mirzaei, M.; Rooholamini, H.; Hassani, A. Effect of rice husk ash and macro-synthetic fibre on the properties of self-compacting concrete. *Constr. Build. Mater.* **2018**, *175*, 371–380. [[CrossRef](#)]
45. Le, H.T.; Ludwig, H.-M. Effect of rice husk ash and other mineral admixtures on properties of self-compacting high performance concrete. *Mater. Des.* **2016**, *89*, 156–166. [[CrossRef](#)]
46. Chopra, D.; Siddique, R.; Kunal. Strength, permeability and microstructure of self-compacting concrete containing rice husk ash. *Biosyst. Eng.* **2015**, *130*, 72–80. [[CrossRef](#)]
47. Zhao, W.; Ji, C.; Sun, Q.; Gu, Q. Preparation and Microstructure of Alkali-Activated Rice Husk Ash-Granulated Blast Furnace Slag Tailing Composite Cemented Paste Backfill. *Materials* **2022**, *15*, 4397. [[CrossRef](#)]
48. Amin, M.N.; Ahmad, W.; Khan, K.; Sayed, M.M. Mapping Research Knowledge on Rice Husk Ash Application in Concrete: A Scientometric Review. *Materials* **2022**, *15*, 3431. [[CrossRef](#)]
49. Zareei, S.A.; Ameri, F.; Dorostkar, F.; Ahmadi, M. Rice husk ash as a partial replacement of cement in high strength concrete containing micro silica: Evaluating durability and mechanical properties. *Case Stud. Constr. Mater.* **2017**, *7*, 73–81. [[CrossRef](#)]
50. Ahmed, A.; Ameer, S.; Abbas, S.; Abbass, W.; Razzaq, A.; Mohamed, A.M.; Mohamed, A. Effectiveness of Ternary Blend Incorporating Rice Husk Ash, Silica Fume, and Cement in Preparing ASR Resilient Concrete. *Materials* **2022**, *15*, 2125. [[CrossRef](#)]
51. Shcherban', E.M.; Stel'makh, S.A.; Beskopylny, A.N.; Mailyan, L.R.; Meskhi, B.; Varavka, V.; Beskopylny, N.; El'shaeva, D. Enhanced Eco-Friendly Concrete Nano-Change with Eggshell Powder. *Appl. Sci.* **2022**, *12*, 6606. [[CrossRef](#)]
52. Nduka, D.O.; Olawuyi, B.J.; Fagbenle, O.I.; Fonteboa, B.G. Assessment of the Durability Dynamics of High-Performance Concrete Blended with a Fibrous Rice Husk Ash. *Crystals* **2022**, *12*, 75. [[CrossRef](#)]
53. Zhang, Z.; Liu, S.; Yang, F.; Weng, Y.; Qian, S. Sustainable high strength, high ductility engineered cementitious composites (ECC) with substitution of cement by rice husk ash. *J. Clean. Prod.* **2021**, *317*, 128379. [[CrossRef](#)]
54. Beskopylny, A.N.; Stel'makh, S.A.; Shcherban', E.M.; Mailyan, L.R.; Meskhi, B.; Smolyanichenko, A.S.; Beskopylny, N. High-Performance Concrete Nanomodified with Recycled Rice Straw Biochar. *Appl. Sci.* **2022**, *12*, 5480. [[CrossRef](#)]
55. Goodman, B.A. Utilization of waste straw and husks from rice production: A review. *J. Bioresour. Bioprod.* **2020**, *5*, 143–162. [[CrossRef](#)]
56. Hidalgo, S.; Soriano, L.; Monzó, J.; Payá, J.; Font, A.; Borrachero, M.V. Evaluation of Rice Straw Ash as a Pozzolanic Addition in Cementitious Mixtures. *Appl. Sci.* **2021**, *11*, 773. [[CrossRef](#)]
57. Shcherban', E.M.; Stel'makh, S.A.; Beskopylny, A.; Mailyan, L.R.; Meskhi, B. Influence of Mechanochemical Activation of Concrete Components on the Properties of Vibro-Centrifugated Heavy Concrete. *Appl. Sci.* **2021**, *11*, 10647. [[CrossRef](#)]
58. Stel'makh, S.A.; Shcherban', E.M.; Beskopylny, A.N.; Mailyan, L.R.; Meskhi, B.; Butko, D.; Smolyanichenko, A.S. Influence of Composition and Technological Factors on Variotropic Efficiency and Constructive Quality Coefficients of Lightweight Vibro-Centrifuged Concrete with Alkalized Mixing Water. *Appl. Sci.* **2021**, *11*, 9293. [[CrossRef](#)]
59. Beskopylny, A.N.; Stel'makh, S.A.; Shcherban', E.M.; Mailyan, L.R.; Meskhi, B.; Varavka, V.; Beskopylny, N.; El'shaeva, D. A Study on the Cement Gel Formation Process during the Creation of Nanomodified High-Performance Concrete Based on Nanosilica. *Gels* **2022**, *8*, 346. [[CrossRef](#)] [[PubMed](#)]
60. Beskopylny, A.N.; Shcherban', E.M.; Stel'makh, S.A.; Mailyan, L.R.; Meskhi, B.; Evtushenko, A.; Varavka, V.; Beskopylny, N. Nano-Modified Vibrocentrifuged Concrete with Granulated Blast Slag: The Relationship between Mechanical Properties and Micro-Structural Analysis. *Materials* **2022**, *15*, 4254. [[CrossRef](#)] [[PubMed](#)]
61. Stel'makh, S.A.; Shcherban', E.M.; Beskopylny, A.N.; Mailyan, L.R.; Meskhi, B.; Beskopylny, N.; Dotsenko, N.; Kotenko, M. Nanomodified Concrete with Enhanced Characteristics Based on River Snail Shell Powder. *Appl. Sci.* **2022**, *12*, 7839. [[CrossRef](#)]
62. GOST 30744 Methods of Testing with Using Polyfraction Standard Sand. Available online: <https://docs.cntd.ru/document/1200011363> (accessed on 12 August 2022).
63. GOST 10180 Concretes. Methods for Strength Determination Using Reference Specimens. Available online: <https://docs.cntd.ru/document/1200100908> (accessed on 12 August 2022).
64. GOST 24452 Concretes. Methods of Prismatic, Compressive Strength, Modulus of Elasticity and Poisson's Ratio Determination. Available online: <https://docs.cntd.ru/document/9056198> (accessed on 12 August 2022).
65. Kuznetsov, D.V.; Kostitsyn, M.A.; Konyukhov, Y.V.; Mitrofanov, A.V.; Lysov, D.V.; Yudin, A.G.; Muratov, D.S.; Burmistrov, I.N. Development of a procedure for modifying nanomaterials of mullite-corundum mixes in equipment with a high-intensity rotating electromagnetic field. *Refract. Ind. Ceram.* **2012**, *53*, 54–58. [[CrossRef](#)]
66. Pourghahramani, P.; Forssberg, E. Comparative study of microstructural characteristics and stored energy of mechanically activated hematite in different grinding environments. *Int. J. Mineral. Process.* **2006**, *79*, 120–139. [[CrossRef](#)]